An Automotive High-Frequency Coreless Transformer of 11kw Dual Active Bridge Converter

Valentin Rigot, Tanguy Phulpin, Jihen Sakly, Daniel Sadarnac

An Automotive High-Frequency Coreless Transformer of 11kw Dual Active Bridge Converter

Valentin Rigot[1,2], Tanguy Phulpin[1], Jihen Sakly[2], Daniel Sadarnac[1]

[1] Université Paris-Saclay, CentraleSupélec, CNRS, Laboratoire de Génie Electrique et Electronique de Paris, France

[2] Vedecom, France

Corresponding author: Valentin Rigot, valentin.rigot@centralesupelec.fr

The Power Point Presentation will be available after the conference.

Abstract

This paper proposes a Dual Active Bridge converter operating at 1.5 MHz switching frequency for an 11kW bidirectional On-Board Charger (OBC) for Electrical Vehicle (EV) application. An air-core transformer is exploited for high-efficiency requirements and for high power density challenge. In addition, a 650 V GaN device was adopted since it is very suitable for this range of voltage and high frequency application. A study on switching frequency application in addition to the voltage range was presented before determining the soft-switching operating area. The required dead time and capacitance are evaluated and presented in this paper. A prototype was implemented, and experiments validate the theoretical results. The converter designed performed at this frequency in soft switching and results exhibits 96% of efficiency with a power density of 6kW/L. These experiments confirm the simulation result and the analytical calculations and further improvements are expected to increase again the power density in the future.

1 Introduction

Emergent issues of electric mobility require higher performances for electric vehicles going through the best power density of power electronics to enlarge the battery space, responsible for the autonomy. The usual way to improve power density is to raise the switching frequency to reduce passive component size [1]. A balance must be found between efficiency and power density due to the frequency losses, especially with the transformer design. The air-core transformer used with a wide bandgap transistor such as GaN transistors is a relevant option to displace the frequency loss contribution and to design a converter with higher power density [2]. Bidirectional converters are required from now on in order to ensure grid sustainability with renewable and intermittent production of electricity as known as grid to vehicle (G2V) and vehicle to grid (V2G) power flows. The low requirement on the passive component makes the Dual Active Bridge (DAB) an adapted topology for exploiting the air-core transformer [3]. The wide bandgap transistor commutes faster than the usual transistor and opens a higher frequency range of soft switching operation which is required for efficiency issues. A DAB converter simulation inducing a soft-switching control is verified by a prototype realized with a ready-to-use GaN inverter branch. The results are experimentally validated with several power range of application. At the end some ideas are proposed to increase again the power density in future applications. Usual bidirectional on-board chargers are required for 22kW power transfer, the presented converter is part of a two cells parallelized converters as shown in ***Fig.1.***

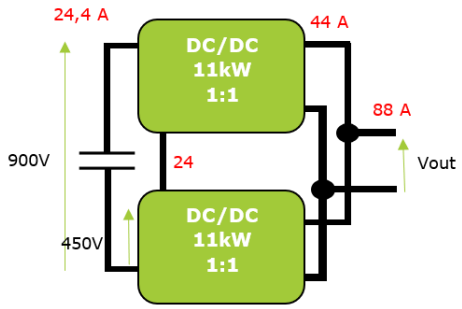

Fig. 1 DC-DC cells arrangement for 22kW charger.

2 Air-core transformer properties

The use of an air-core transformer is relevant for higher frequency because of the lack of saturation of the magnetic core and no loss of eddy current or hysteresis. In a previous study [4], a new geometry of air-core transformer was developed to fit automotive usual power transfer. This transformer compensates for the few magnetizing inductance and coupling coefficient by a special winding arrangement. To make the best use of this component, the design of the converter considers the transformer values as a determined value.
The equivalent circuit of the transformer chosen for the characterisation is presented ***Fig.2.***

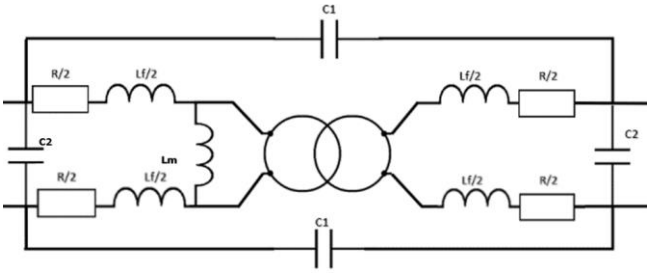

Fig. 2 Equivalent circuit of the air core transformer

The equivalent electrical values and the mechanicals results are given in Table 1 and the resistance is approximated by a polynomial form given by impedance analyzer.

Transformer $(n = 1)$	
$L_m(\mu H)$	20,6
$L_k(\mu H)$	1,5
$R(m\Omega) \quad (f(kHz))$	$8.10^{-5}\, f^2 - 0{,}0427\, f + 112{,}26$
$C_1(\mu F)$	$f(kHz)$
$C_2(\mu F)$	$f(kHz)$
$V(L)$	$f(kHz)$
$M(kg)$	$f(kHz)$

Table 1 Electricals and mechanicals properties of the air-core transformer

The magnetizing and leakage inductances values $L_m$and L_k are low and require high frequency to operate at higher power which corresponds to our application. n is the turn ratio, R the resistance and *f* the switching frequency.

3 Topology determination

The automotive context imposes isolated topology to reduce touch current hazard. Moreover, the bidirectional properties needed for the converter restrict the study to the CLLC resonant converter [5] or those hybrid [6] and the Dual Active Bridge phase shift converter. The CLLC Voltage gain transfer function is written in (1):

$$\frac{V_{out}}{V_{in}} = \frac{f^2(m-1)}{\sqrt{(mf^2-1)^2 + f^2(f^2-1)^2(m-1)^2Q^2}} \quad (1)$$

Where f is the frequency ratio from the resonance value, m is the inductance ratio as in (2) and Q the quality factor as in (3).

$$m = \frac{L_m + L_k}{L_k} \quad (2)$$

$$Q = \frac{n^2\pi^2 P\sqrt{L_r}}{8{V_{out}}^2\sqrt{C_r}} \quad (3)$$

The designed transformer imposes a m value of 14.7. According to (1) and (3), the worst case of operation is for the light load at V_{outmin}. A computer aided calculation to plot the minimum power transfer for different frequency range is shown in ***Fig.3***.

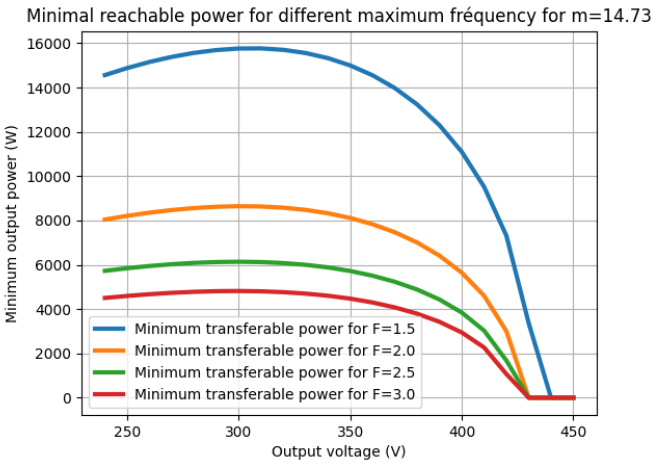

Fig. 3 Minimum transferable power in a CLLC topology for the designed transformer

The designed transformer imposes a maximum frequency superior to 3 times higher than the resonant frequency to ensure light loads without designing an additional air core series inductance. This solution is not suitable in our application because for optimizing the power density, our leakage inductance is considered in our transformer without any additional inductance. The dual active bridges power transfer function is written in (4) [7].

$$P_{out}(d) = \frac{(1-|d|).d}{2.n.f.L_k}.V_{in}.V_{out} \qquad (4)$$

Where P_{out} is the transferred power, V_{in} and V_{out} are the input and output voltage, and d is the phase shift that controls the power flow.
This topology looks relevant for our application by considering its low requirement on the magnetization inductance and because of the constant switching frequency operation, main goal for optimizing the design. The usual electric vehicle voltage range values are defined in our framework between 250V and 450V on the battery side and 450V DC on the grid side. By compiling this requirement with the transformer's properties and the equation (4), the switching frequency of the converter can be determined in (5) thanks to the 11kW maximal power transfer previously define.

$$f = \frac{(1-|d_{max}|).d_{max}}{P_{out,max}.2.n.L_k}.V_{in,max}.V_{out,max} \qquad (5)$$

According to the table 1 and at the determined switching frequency of $1.5MHz$, the transformer exposes a resistance of $228.21\,m\Omega$ if we use the first harmonic approximation assuming a d_{max} of 0.45. This frequency is very high for power transistors, and the difficulty is to ensure the soft switching for maximal efficiency and thermal withstand.

4 Determination of the soft switching area

Soft switching can be achieved when the current crossing the transistor is in the opposite sign from the voltage variation sign of the transistor terminal as shown in ***Fig.4***.

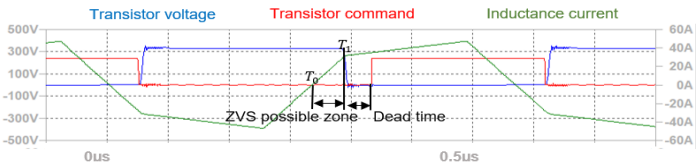

Fig. 4 Soft switching margin in Dual Active Bridge DC-DC converter

The determination of the soft switching limit is achieved when the spontaneous changing sign in the inductance current $I_L(T_0) = 0$ corresponds to the time T_1 when the transistor switch as written in (6) [8].

$$I_L(T_1) = \frac{1}{4.f.L_k}(-V_{in} + (1-2d).V_{out}) + (V_{in} + V_{out})\frac{d}{2.f.L_k} \qquad (6)$$

A calculation of the minimum power transfer in the function of the output voltage can be computed with the calculation of soft switching minimal phase shift d and is exposed in ***Fig.5***.

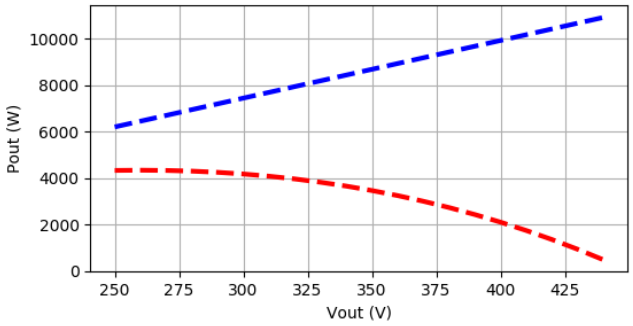

Fig. 5 Soft switching area in the function of output power and voltage for $V_{in} = 450V$: Red: ZVS limit, Blue: maximal power

Moreover, a minimal deadtime corresponding to the natural capacitance discharge of the transistor is necessary. The computing of the required deadtime t_{dt} for each period depends on the transistor C_{oss} values and can be written as (4). It becomes possible to isolate this value and to determine the necessary dead time to keep ZVS switching active as in (5) [9].

$$I_L(T_1) > \frac{2.C_{oss}.V_{out}}{t_{dt}} \qquad (7)$$

$$t_{dt} > \frac{C_{oss}.V_{out}}{(-V_{in}+(1-2.d).V_{out})+(V_{in}+V_{out})} . \frac{d}{4.f^2.L_k{}^2} \quad (8)$$

5 Input and output capacitance

Due to high switching frequency, the output voltage ripples require some lower capacitance values and size. Ceralink capacitances are used for their low volume and stability. The Dual active bridge output voltage ripple ΔV_{out} can be expressed as (9)[10].

$$\Delta V_{out} = \frac{[V_{out} + (2d^2 - 1)nV_{in}]^2}{32f^2 L_k C(V_{out} - nV_{in})} \quad (9)$$

For a 1% ripple tolerance (4.5V max), a 9µF capacitance is Suitable to ensure a power transfer of 11kW with less than 1% of output voltage ripple. The result of this capacitance value is shown in ***Fig.6***.

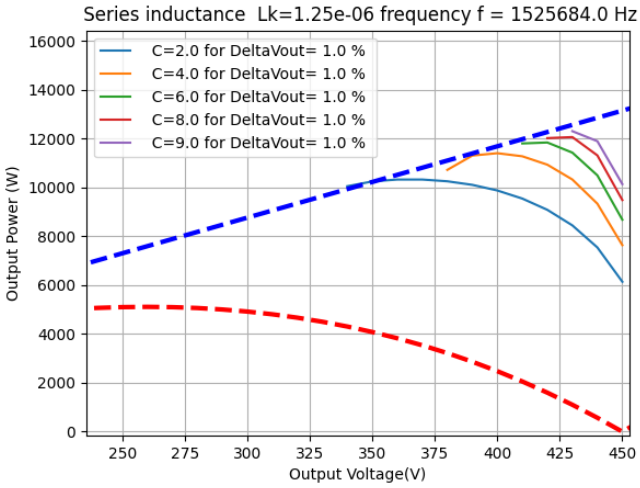

Fig. 6 1% output oscillation limit for different output capacitance value.

The symmetrical properties of the converter ensure the same voltage ripple in reverse power flow. The input capacitances are also chosen of 9µF.

6 Converter realization

A GaN ready-to-use inverter branch from GaN system GSP65R13HB-EVB is selected to ensure the best power density even if a specific design can improve again the total power density. The transformer is linked to the inverter branch by the mechanical 3D printed transformer support. A PCB motherboard was realized to limit parasitic elements and to connect a low-voltage power supply, sensors input and output capacitance and control card command as shown in ***Fig.7***.

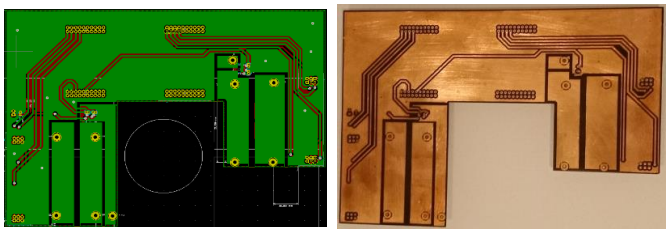

Fig. 7 PCB motherboard : left :KiCAD design; Right : Realized PCB

This motherboard is set between the command board and the inverter branch. Its aimed is to distribute clearly the PWM command and also to connect high sides and low sides on both primary and secondary sides of the transformer. The final architecture of the converter is presented in ***Fig.8***.

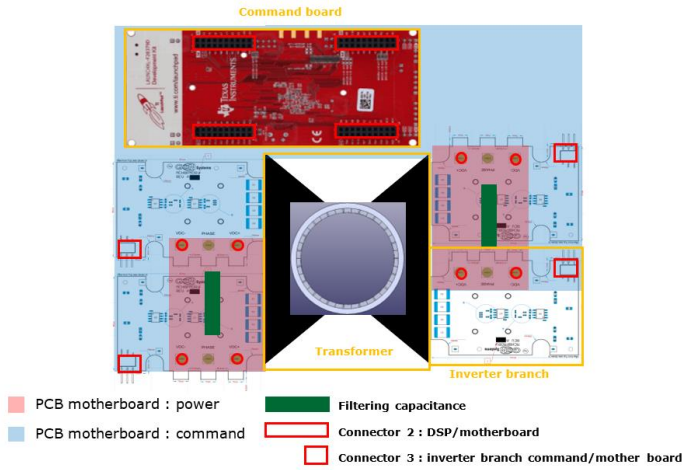

Fig. 8 schema of the architecture of the final converter

Finally, the thermal study of the transformer required forced cooling realized by a fan under the transformer.

7 Results

The converter assembly result in the ***Fig.9***.The addition of the volume of each part leads to a power density of 6.6kW/L by considering the heatsinks for 7 kW according to Table 2. The gain in weight is also fundamental for embedded systems. The proposer transformer present a reduction of 250g passing from 497g to 240,6g compared to a state of the art ferrite transformer. In globality, the converter weights less than 1kg according to Table 3.

	$Volume\ (cm^3)$	$Power\ density\ (kW/L)$
$Transformer\ +cooling$	$6 * 6 * 8.1$	30.87
$Inverter\ branch\ +cooling$	$4 * 3{,}6 * 5.5 * 4$	28.40
$PCB + DSP$	$15 * 20 * 1.5$	20
$Total$	1058.4	6.61

Table 2 Volume in the converter's parts

	$Weight\ (g)$	$Power\ to\ weight\ ratio\ (kW/kg)$
$Transformer$	240.6	37.41
$Inverter\ branch\ +cooling$	$4 * 131$	17.17
$PCB + DSP$	$55 + 61$	77.58
Fan	66.2	135.95
$Total$	948	9.5

Table 3 Weight in the converter's parts

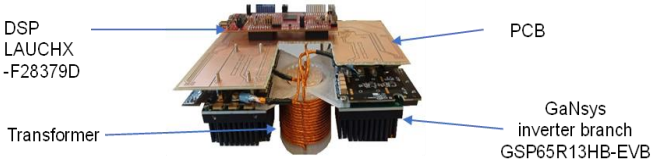

Fig. 9 Air core transformer dual active bridges DC-DC converter prototype

Measurements permit to trace the efficiency for various output power and several output voltages (***Fig.10***). It leads to comparing with the result in the soft switching area transposed from ***Fig.5*** to ***Fig.10***. For a lower power, less than 5kW, the efficiency is estimated at around 90% but for more power, such as the main use of the converter, the converter reaches 96% for a wide voltage range going from 360V to 460V, in both cases of power transfer (V2G and G2V).

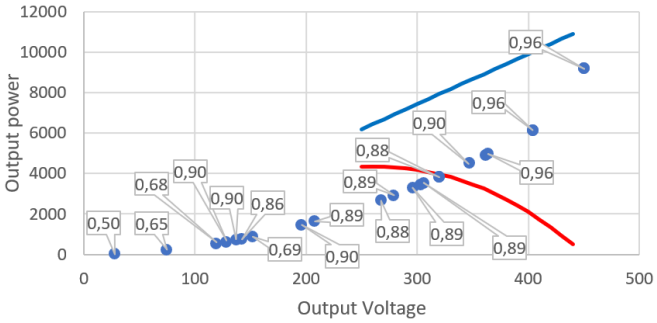

Fig. 10 Tested functional points regarding the efficiency and soft switching area

7.1 Conclusion

An 11kW converter was designed and tested until 9 kW. It reaches an efficiency of 96% at 1.5MHz for a wide range of voltage. This converter shows a power density of 6kW/L although this value can be easily improved by a unique dedicated PCB development included command, transistors, transformer, and capacitance. It can also be improved by reviewing the thermal design of the inverter branch which are prototyping devices with tests materials such as the DSP or increase the power transfer to 11kW.

8 References

[1] J. Biela, U. Badstuebner and J. W. Kolar, "Impact of Power Density Maximization on Efficiency of DC-DC Converter Systems," in IEEE Transactions on Power Electronics, vol. 24, no. 1, pp. 288-300, Jan. 2009, doi: 10.1109/TPEL.2009.2006355.

[2] A. Jafari, M. S. Nikoo, N. Perera, H. K. Yildirim, F. Karakaya, R. Soleimanzadeh, an d E. Matioli "*Comparison of Wide-band-gap Te chnologies for Soft-Switching Losses at High F requencies",* in *IEEE Transactions on Power Electronics*, vol. 35, no. 12, pp. 12595-12600, Dec. 2020, doi: 10.1109/TPEL.2020.2990628

[3] Y. Du, S. Lukic, B. Jacobson and A. Huang, "Review of high power isolated bi-directional DC-DC converters for PHEV/EV DC charging infrastructure," *2011 IEEE Energy Conversion Congress and Exposition*, 2011, pp. 553-560, doi: 10.1109/ECCE.2011.6063818.

[4] V. Rigot, T. Phulpin, D. Sadarnac and J. Sakly, *A new design of an air core transformer for Electric Vehicle On-Board Charger, 2020 22nd European Conference on Power Electronics and Applications (EPE'20 ECCE Europe),* 2020, pp. 1-9

[5] Infineon "Resonant LLC Converter: Operation and Design 250W 33Vin 400Vout Design Example" Application Note AN 2012-09 Sept. 2012

[6] L. Sobrayen, C. Karimi, P. Dehem, T. Phulpin, D. Sadarnac. "Elimination of Circulating Current in Wide Range LLC Resonant Converter with a Hybrid Bridge and Simultaneous PWM and PFM Control," *2021 IEEE Applied Power Electronics Conference and Exposition (APEC)*, Jun 2021, Phoenix (virtual), United States. pp.327-334, ⟨10.1109/APEC42165.2021.9487389⟩

[7] P. He and A. Khaligh, "Comprehensive Analyses and Comparison of 1 kW Isolated DC–DC Converters for Bidirectional EV Charging Systems," in IEEE Transactions on Transportation Electrification, vol. 3, no. 1, pp. 147-156, March 2017, doi: 10.1109/TTE.2016.2630927.
[8] M. Blanc, Y. Lembeye, JP Ferrieux *Dual Active Bridge pour la conversion continu-continu, techniques de l'ingénieur,* Feb. 2019
[9] C. Mi; H. Bai; C.Wang; S. Gargies, *Operation, design and control of dual H-bridge-based isolated bidirectional DC–DC converter* Volume 1, Issue 4, December 2008, p. 507 – 517 DOI: 10.1049/iet-pel:20080004
[10] G. G. Oggier, R. Leidhold, G. O. Garcia, A. R. Oliva, J. C. Balda and F. Barlow, "Extending the ZVS operating range of dual active bridge high-power DC-DC converters," 2006 37th IEEE Power Electronics Specialists Conference, 2006, pp. 1-7, doi: 10.1109/pesc.2006.1712142.